International Journal of Innovative Computing, Information and Control
Volume **18**, Number **3**, June **2022**

ICIC International ©2022 ISSN 1349-4198
pp. 941–955

ENHANCEMENT FOR LOW-CONTRAST IMAGES WITH FITZHUGH-NAGUMO NONLINEARITY AND ADAPTIVE STOCHASTIC RESONANCE

Dongcheng Wang, Yumei Ma*, Zhenkuan Pan and Ning Zhang

College of Computer Science and Technology
Qingdao University
No. 308, Ningxia Road, Qingdao 266071, P. R. China
{ wdc19970207; nealtoon }@163.com; zkpan@126.com
*Corresponding author: mayumei@qdu.edu.cn

Received November 2021; revised March 2022

Abstract. *In this paper, an iterative model of self-synaptic FitzHugh-Nagumo (FHN) neurons based on adaptive stochastic resonance (ASR) and improved by Euler-Maruyamas method is proposed to enhance the contrast of low-brightness images. Firstly, the stochastic pooling network based on Kalman and least mean square (Kalman-LMS) adaptive algorithm is designed to eliminate noise disturbance in input low contrast image, and the optimal parameter value of self-synaptic FHN nonlinear system is obtained by least square estimation (LSE) adaptive algorithm. Then the self-synaptic FHN neuron nonlinear equation is reconstruct by Euler-Maruyamas iterative method. Finally, the ASR is applied in an iterative manner to combining parameter values of self-synaptic FHN neurons with brightness values of low-contrast images. The optimal response is measured by perceptual quality measurement (PQM), structural similarity index measure (SSIM) and relative contrast enhancement factor (RCEF). However, compared with the existing methods, the image brightness and visual perception are significantly improved by the method proposed in this paper.*

Keywords: Self-synaptic FitzHugh-Nagumo neuron, Stochastic resonance, Adaptive algorithm, Image enhancement

1. **Introduction.** The enhancement of low illumination images is widely used in underwater images [1, 2], edge detection, night vision imaging [3], road crack detection [4], medical imaging [5] and so on. A large number of image enhancement algorithms are based on two-dimensional grayscale image enhancement. The existing low illumination image enhancement methods include gamma correction (Gamma), contrast-limited adaptive histogram equalization (CLAHE), Gaussian Filter, Median Filter, etc. [6, 7]. It is proposed that the excessive enhancement of noise in standard histogram equalization methods is overcome by the CLAHE method [8]. However, the halo artifact is generated around the image by the CLAHE method when there is a high gradient. It is proposed in [9] that the smooth curve is used by gamma correction to automatically enhance the brightness of the image through the weighted distribution. No halo artifacts are generated by this method, but the degree of image enhancement is not significant. These methods of image enhancement are also applied to low-illuminance color images in the red-green-blue (R-G-B) space [10-12]. Jobson et al. [13] proposed single-scale retinex (SSR) and multi-scale retinex (MSR) theory that the contrast of the image can be moderately enhanced by balancing in three aspects: edge enhancement, dynamic range compression and color steadiness. However, the effect of the image enhancement is not ideal by the

DOI: 10.24507/ijicic.18.03.941

SSR algorithm. And the MSR algorithm is computationally intensive. While the image is enhanced, the edge of the image is blurred, resulting in the loss of some details.

Beyond that, the nonlinear phenomenon of stochastic resonance (SR) was introduced by Benzi that the weak signal would be enhanced by adding an appropriate amount of noise [14, 15]. And the research of SR has been applied in many fields such as image processing [16-25]. In recent years, adaptive stochastic resonance (ASR) has also been discovered and developed rapidly [26]. It has been widely used in the fields of ultraviolet absorption spectroscopy, fault detection and signal processing [27-30]. It is proposed that the optimal parameters of the ASR system are adaptively selected by constructing an improved particle swarm optimization algorithm and improved signal-to-noise ratio index [31]. By this method the ability of weak signal feature extraction is improved effectively, and it is well used in fault detection. It is proposed that the contrast of low brightness images can be improved by an analysis method based on stochastic resonance and spatial domain [32]. The contrast of the image is improved by associating the brightness value of the image with the parameters of the nonlinear system. It shows high performance in visual perception and color naturalness. After that, an iterative method based on wavelet fusion and ASR is proposed to enhance the contrast of low brightness images [33]. However, the uniform low contrast images are significantly enhanced and the uneven illumination images are not enhanced as well as desired by these methods. In addition to the research on bistable nonlinearities, there are also many researches on weak signal enhancement based on FitzHugh-Nagumo (FHN) neuron nonlinearities [34-36]. The FHN neuron model is a simplified Hodgkin-Huxley (H-H) model. Because of its simple calculation and rich electrophysiological properties, it is widely used in the research of stochastic resonance [37, 38]. Although more effective results have been achieved, some details are often lost as the self-synaptic feedback structure of neurons is not taken into account. At present, the non-negligible role of self-feedback structure in cranial nervous system has been confirmed by a large number of studies [39, 40]. It is precise to consider the role of self-synaptic structure in image enhancement of FHN neuron nonlinearities.

With the continuous development and progress of medical imaging and night detection, a large number of contrast image enhancement methods have appeared. However, the desired results cannot be obtained by existing methods. In this paper, an iterative model of self-synaptic FHN neurons based on ASR for enhancement of low brightness images has been presented. The Euler-Maruyamas iterative method is used to reconstruct the traditional FHN and self-synaptic FHN equations. The Kalman and least mean square (Kalman-LMS) adaptive algorithm is selected to eliminate the input signal interference term and the least square estimation (LSE) adaptive algorithm is selected to obtain the optimal system parameters. All areas of the original image are processed appropriately by controlling the number of iterations and iteration steps. The experiments of image enhancement are carried out for three types of low brightness images with different pixel sizes. The experimental results show that the contrast of low brightness images is improved effectively. And the color naturalness of the original image has been maintained by the self-synaptic FHN neuron model based on ASR. Compared with traditional methods, the effect of the contrast enhancement is more significant, and the halo artifact is not caused by excessive noise enhancement. As the relative contrast enhancement factor (RCEF) and the perceptual quality measurement (PQM) indicators of the method proposed in this paper are calculated and measured after each iteration, low brightness images of different sizes have been enhanced effectively through iteration.

The rest of the paper is organized as follows. In Section 2, it introduces the experimental procedures we proposed, the principle of adaptive stochastic resonance, parameter selection process through adaptive algorithm and performance indicators. In Section 3,

the experimental results and performance analysis comparisons of five classical methods and self-synaptic FHN neuron model are given to prove the effectiveness of the methods we proposed. Finally, conclusion is provided in Section 4.

2. FHN Neuron Model and Performance Evaluation.

2.1. **Experimental process.** Since the low-contrast images are not enhanced significantly by existing enhancement methods, a new method based on self-synaptic FHN neurons and adaptive stochastic resonance is proposed in this paper. The Euler-Maruyamas iterative method is used to reconstruct the traditional FHN and self-synaptic FHN equations. Three adaptive algorithms are selected to obtain the optimal system parameters. The experimental flowchart is shown in Figure 1. The main steps of self-synaptic FHN neuron model based on ASR to enhance low-contrast images are as follows.

Step1. Convert original low-contrast images from red-green-blue (RGB) space to hue-saturation-value (HSV) space through MATLAB functions. The subsequent operations of this conversion only need to process the V-direction component, which preserves the hidden color of the original low brightness image.

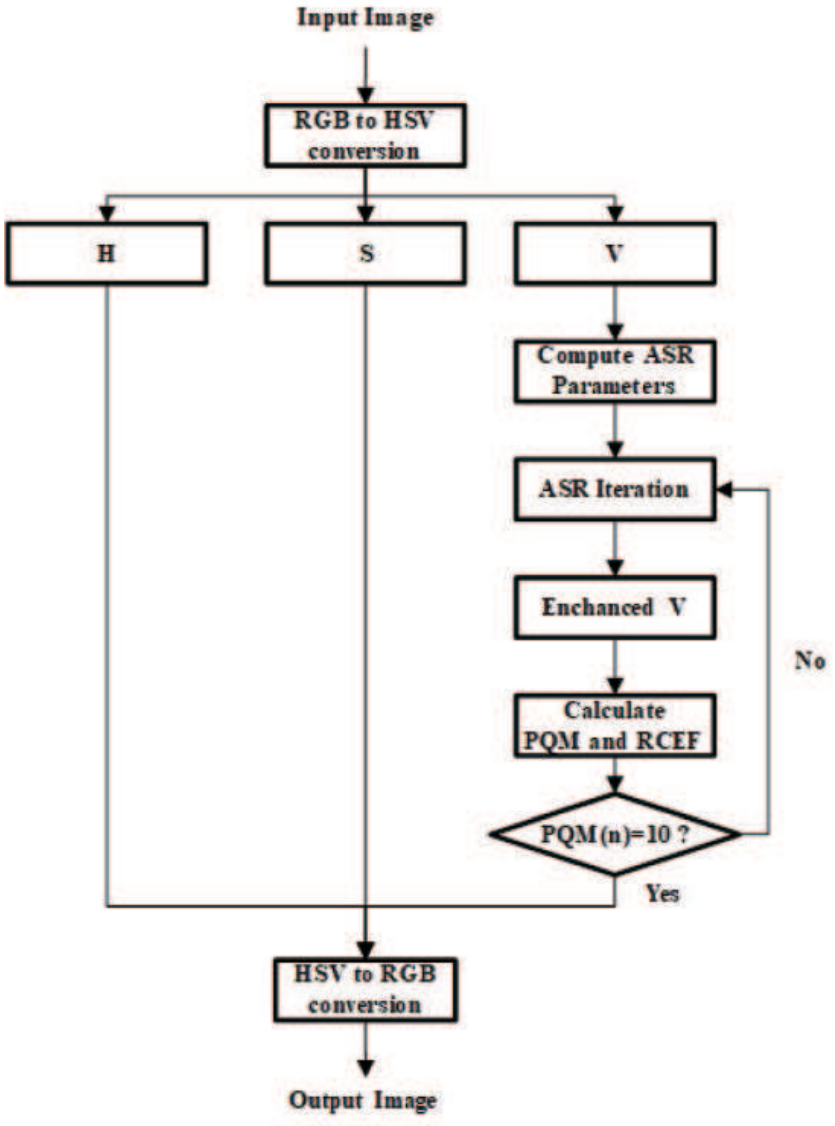

FIGURE 1. Flowchart of ASR-based enhancement algorithm on contrast

Step2. The optimal parameters determined by adaptive algorithm. The Kalman-LMS adaptive algorithm is proposed to eliminate the noise disturbance in the input image, and the optimal parameters of self-synaptic FHN nonlinear system are obtained by the LSE adaptive algorithm.

Step3. Adaptive iteration. The Euler-Maruyamas iterative model of FHN neurons with optimal parameters is used to adjust the brightness values of input low-contrast images. After each iteration, *RCEF* and *PQM* of neuron output are calculated and updated. On the premise that the *PQM* is as close to 10 as possible, iterations are carried out until the *RCEF* reaches its maximum value.

Step4. Convert enhanced images from HSV space to RGB space. The enhanced lightness vector, x, is combined with the saturation vector and hue vector of the original low-illumination image and the enhanced color image is obtained by converting it back to the RGB color space through the MATLAB function.

2.2. **Self-synaptic FHN neuron model.** The existence of stochastic resonance in biological neurons has been proven by a large number of experiments [41, 42]. In this paper, a new model of FHN neurons is used to enhance the image from low-illumination state to high-illumination state after a certain number of iterations. A classic FHN neuron dynamic system is modelled as follows:

$$\frac{dx}{dt} = x(\alpha - x)(x-1) - \frac{\beta}{\gamma}x + s_{(t)} + \xi_{(t)} \tag{1}$$

where x is the rapidly changing variable of membrane voltage, α is the threshold value for $\alpha \in (0,1)$, γ is a positive constant, β is a positive constant that reflects the effect of a slowly changing variable on the system, $s_{(t)}$ stands for driving force input, and $\xi_{(t)}$ is the external added noise. Stochastic differential Equation (1) can be reconstructed by the Euler-Maruyamas iterative method as follows [43]:

$$x(n+1) = x(n) + \Delta t\left(x(n)(\alpha - x(n))(x(n)-1) - \frac{\beta}{\gamma}x(n) + I_{input}\right) \tag{2}$$

where Δt denotes the iteration step size and $I_{input} = s_{(t)} + \xi_{(t)}$ stands for input signal.

In addition to the traditional FHN neuron model, we also consider the self-synaptic structure of the neuron itself. The self-synaptic FHN neuron model is shown below:

$$\frac{dx}{dt} = x(\alpha - x)(x-1) - \frac{\beta}{\gamma}x + s_{(t)} + \xi_{(t)} - I_{aus} \tag{3}$$

$I_{aus} = E(x(t) - x(t-\tau))$ is self-synaptic current where τ denotes the time delay and E stands for self-synaptic conductivity coefficient. Stochastic differential Equation (3) also can be reconstructed by the Euler-Maruyamas iterative method as follows:

$$x(n+1) = x(n) + \Delta t\left(x(n)(\alpha - x(n))(x(n)-1) - \frac{\beta}{\gamma}x(n) + I_{input} + E(x(n-1))\right) \tag{4}$$

where Δt is the self-synaptic iteration step size. In this paper, I_{input} is the pixel value of the input low-illuminance image with external Gaussian white noise. When $E = 0.46$, the image is best enhanced by consulting a large number of literature and combining with the experimental data in this paper [44, 45].

2.3. **System parameters selection through adaptive algorithm.** In this section, the optimal parameters of the self-synaptic FHN neuron model are obtained by the Kalman-LMS and LSE adaptive algorithm [46, 47]. According to (2) and (4), the stochastic resonance phenomenon appears as selecting the appropriate FHN and self-synaptic FHN parameters α, β, and γ. The parameters β and γ are found to be proportional

through observation, assuming $\gamma = 1$. The main research focus of this section is that the parameters α and β of the FHN neuron model are obtained by Kalman-LMS and LSE adaptive algorithm. The process of parameter optimization by the Kalman-LMS and LSE adaptive algorithm in the Pooling network is as follows.

Step1. Multi-threshold quantization processing. Random Gaussian white noise is added to the input signal x and the output of each subsystem node y_n can be obtained by transforming the following nonlinear node function $f(x)$.

$$f(x) = \begin{cases} 1, \ x + \eta_n > \delta \\ 0, \ x + \eta_n \leq \delta \end{cases} \tag{5}$$

where η_n is Gaussian white noise with a mean of 0. δ is the threshold of the network node, $\delta = 0$.

Step2. Calculate and update weight error covariance matrix and weight vector. The network output and optimal learning gain after each iteration are calculated, then the weight error covariance matrix and weight vector are updated.

The network output $\hat{x}_n$ of each iteration is as follows:

$$\hat{x}_n = W_n^T y_n + W_0 \tag{6}$$

where W_n denotes the weight vector after each iteration. The weight W_0 is initialized as a zero matrix of $M * M$.

The optimal learning gain g_n after each iteration is as follows [48]:

$$g_n = G_n \tilde{y}_n = \frac{\Phi(n)\tilde{y}_n}{\tilde{y}_n^T \Phi(n) \tilde{y}_n + \sigma_n^2} \tag{7}$$

where G_n is the Kalman gain. $\Phi(n)$ is the weight error covariance matrix. $\Phi(0) = \sigma^2 I$, I denotes the identity matrix and σ^2 is a positive value. σ_n^2 is the variance of externally added Gaussian white noise, $\sigma_n^2 = 0.01$. $\tilde{y}_n$ is the observed value of y_n.

$$\tilde{y}_n = y_n - E[y_n] \tag{8}$$

The error e_n and the mean square error J of network output and network input are calculated. The calculation method of error e_n is as follows:

$$e_n = \hat{x}_n - x \tag{9}$$

The calculation method of mean square error J is as follows:

$$J = E\left[{e_n}^2\right] \tag{10}$$

The value of J is calculated at the end of each iteration and judged whether it reaches the minimum value. If the minimum value is not reached, the weight vector and the weight error covariance matrix need to be updated. The weight vector is updated each time as follows:

$$W_{n+1} = W_n + g_n \left(\tilde{x}_n - W_n^T \tilde{y}_n\right) \tag{11}$$

where $\tilde{x}_n$ is the observed value of x_n. And the weight error covariance matrix is updated as follows:

$$\Phi(n+1) = \Phi(n) - g_n \tilde{y}_n^T \Phi(n) \tag{12}$$

The estimated value $\hat{x}$ of the input signal after noise elimination is obtained by summing up all the iterative network outputs.

$$\hat{x} = \sum_{n=0}^{N} \hat{x}_n \tag{13}$$

Step3. Calculate ASR parameters. The estimated value of the input signal after noise elimination is taken as the independent variable, and the expected output as the dependent variable. The optimal system parameters α and β are obtained by fitting the least square estimation (LSE) algorithm.

Since the perturbation term is a random error that cannot be measured, the optimal parameters solution of the self-synapse FHN neuron model is slightly changed after adaptive iterative processing. The average values are selected as the system parameters of the self-synaptic FHN neuron model after a large number of experiments, $\alpha = 0.1041$ and $\beta = 0.0838$.

2.4. **Image performance evaluation indicator.** Existing image evaluation methods such as mean square error (MSE), peak signal-to-noise ratio (PSNR), quality index, and structural similarity index measure (SSIM) which require reference images or undistorted images are not suitable for our experimental study. Because the image contrast as well as perceptual quality are needed to be the measure performance, three indicators are selected to measure image performance: the distribution separation measure (DSM), perceptual quality measurement (PQM) and relative contrast enhancement factor (RCEF).

The measurement of RCEF is based on the mean and global variance of the observed low-illumination images and the enhanced high-illumination images. It can be said that when the structure of the image is clearer and the contrast of the image is enhanced, the enhancement value can be illustrated by the Michelson contrast index [49], which can be summarized as the contrast quality index C

$$C(v) = \frac{{\sigma_v}^2}{\mu_v} \tag{14}$$

where σ^2 and μ are, respectively, the global variance and mean of image v. In addition, it is demonstrated that an enhanced image, with increasing of structural characteristics, brightness and edge, is connected with increasing values of contrast quality index. By calculating the observed image C_I and the contrast quality value of the enhanced image C_O, their ratio is called the relative contrast enhancement factor (RCEF) [50], as shown below:

$$RCEF = \frac{C_O}{C_I} \tag{15}$$

Taking account of the blur artifacts and visible blocks of the image, a non-referenced perceptual quality evaluation method is used for the evaluation of image perceptual quality, which we call perceptual quality measurement (PQM) as follows [51]:

$$PQM = a + b\beta^{r_1}\alpha^{r_2}\gamma^{r_3} \tag{16}$$

where a, b, r_1, r_2 and r_3 are the model parameters of the test data estimated by subjective estimation method as described by [49] ($a = -245.9$, $b = 261.9$, $r_1 = -0.0240$, $r_2 = 0.0160$ and $r_3 = 0.0064$). β is the average blockiness, used to evaluate the average difference between the block boundaries of the vertical and horizontal characteristics. α and γ are used to evaluate the activity of image pixels. Although it is difficult to evaluate an unclear image without a reference, it can lead to a reduction in signal activity, while combining the blockiness and signal to highlight the relative blur of the image. γ denotes the zero-crossing rate and α denotes the average absolute difference of pixels in the image block. According to Mukherjee and Mitra [52], the difference between PQM and 10 should be as close to zero as possible to obtain the best perceived quality.

The DSM [53] indicator is selected to measure the changes between the original low-illumination image and the enhanced image, which shows the enhancement degree of the target area compared to its background area as follows:

$$DSM = \left(\left|\mu_e^M - \mu_e^N\right|\right) - \left(\left|\mu_p^M - \mu_p^N\right|\right) \tag{17}$$

where μ_e^M, μ_p^M, μ_e^N, μ_p^N represent the mean of the target area (M) and background area (N) of the enhanced image (e) and the original low-illumination image (p), respectively.

Generally, large values of *RCEF* and *DSM* index imply better visual perception after contrast enhancement of the image. Therefore, in order to obtain the best perceptual quality, we stipulate that we stop the iteration when the difference between *PQM* and 10 is closest to zero, and calculate the *RCEF* and *DSM* values of the enhanced image. For the *DSM* indicator, higher values indicate the greater enhanced degree of the image.

3. **Experimental Results and Performance Analysis.** In order to verify the enhancement effect of self-synaptic FHN neuron model based on ASR reconstructed in this paper for low-illuminance images, three kinds of low-illuminance images with different pixel sizes (128×128, 256×256, 512×512) are selected for enhancement experiments. The variance of external added noise is 0.000001. And five methods such as contrast-limited adaptive histogram equalization (CLAHE), single-scale retinex (SSR), gamma correction (Gamma), Median Filter and Gaussian Filter are selected for experimental comparison. Figures 2(a)-2(c) are the three original images, and Figures 3(a)-3(c) are their corresponding low-illuminance images. (Both sets of images are from the LOL database).

In the actual experiment, the model parameters have been solved in Section 2.3 by Kalman-LMS and LSE adaptive algorithm. The number of iterations required for different images to switch from a low-illuminance state to a high-illuminance state is different.

(a) (b) (c)

FIGURE 2. Original images: (a) A Bookcase image with a pixel size of 128×128; (b) a Chopsticks frame image with a pixel size of 256×256; (c) a Tableware image with a pixel size of 512×512

(a) (b) (c)

FIGURE 3. Low-illuminance images after processing

Three indicators such as *PQM*, *DSM* and *RCEF* are used to measure the effect of image enhancement in this paper.

3.1. **Bookcase image.** In Figure 4, it shows the comparison of the enhancement effect with the five classic methods including CLAHE, SSR, Gamma, Median Filter, Gaussian Filter in Figures 4(c)-4(g), FHN neuron model and the self-synaptic FHN neuron model based on ASR in Figure 4(h) and Figure 4(i) for the image size of 128×128. Obviously, the image enhanced by CLAHE, SSR and Median Filter is not clear, especially the image enhanced by the CLAHE method mixed with large areas of halo artifacts. It shows that the contrast enhancement effect of the image through the ASR iteration method is better than others. The results show that the image enhanced by the ASR iterative method is noiseless.

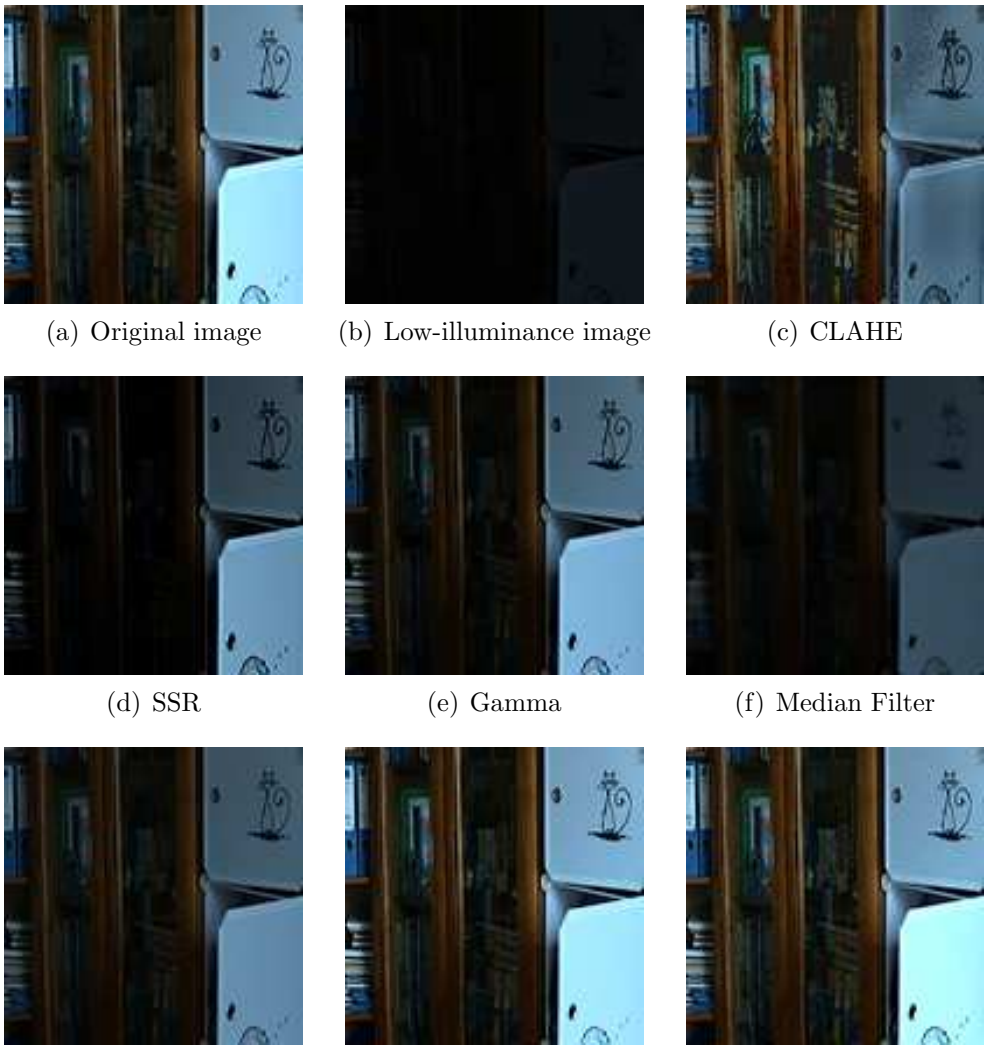

(a) Original image (b) Low-illuminance image (c) CLAHE

(d) SSR (e) Gamma (f) Median Filter

(g) Gaussian Filter (h) FHN (i) Self-synaptic FHN

FIGURE 4. Comparison of Bookcase image with different enhancement methods

Table 1 shows the performance comparison of PQM, RCEF and DSM indicators under different enhancement methods for Bookcase image. As introduced in Section 2.4, the superiority of an image enhancement method mainly depends on the premise that the PQM value is as close as possible to 10, the larger the RCEF index, the better the image enhancement effect. In Table 1, it is shown that the RCEF index of CLAHE is the lowest,

TABLE 1. Performance index of Bookcase image under different enhancement methods

Method	Bookcase image (128 × 128)		
	PQM	RCEF	DSM
CLAHE	9.0380	0.6686	12.1880
SSR	10.6863	3.0836	50.3202
Gamma	10.1255	2.7913	65.1850
Median Filter	10.2288	0.9791	31.6782
Gaussian Filter	10.9663	1.7934	57.3767
FHN	**10.0008**	**3.3191**	**101.0324**
Self-synaptic FHN	**9.9998**	**3.3652**	**106.4402**

$RCEF = 0.6686$. The RCEF index value of the image enhanced by Median Filter and Gaussian Filter is also not ideal. Obviously, the new method is the best in terms of PQM indicators, RCEF indicators and DSM indicators. The RCEF index of our method, especially the self-synaptic FHN neuron model is 3.3652 and $PQM = 9.9998$.

3.2. **Chopsticks frame image.** In Figure 5, it shows the comparison of the enhancement effect with the five classic methods, FHN neuron model and the self-synaptic FHN neuron model based on ASR for the image size of 256×256. It shows that the enhanced images with low contrast are obtained by SSR, Gamma and Median Filter methods. Although the contrast of the image enhanced by CLAHE method is significantly improved, the image has artifacts due to the amplification of noise. The results show that compared with the classic method, the new method has a significant improvement in color naturalness.

Table 2 shows the performance comparison of PQM, RCEF and DSM indicators under different contrast enhancement methods for Chopsticks frame image. It is found from the Table 2 that all performance indicators are significantly lower than those of our method compared to the five traditional methods. The value of the FHN neuron model on the RCEF index is 5.6788 and the self-synaptic FHN neuron model is 5.8378, and their PQM values are, respectively, 10.0032 and 9.9976.

3.3. **Tableware image.** In Figure 6, it shows the comparison of the enhancement effect with the five classic methods, FHN neuron model and the self-synaptic FHN neuron model based on ASR for the image size of 512×512. The results show that the contrast of the image enhanced by SSR is lower than that before. The contrast of the image is not significantly enhanced by Gamma and Median Filter. The contrast of the image is significantly enhanced by the Gaussian Filter method, but it is not as significantly enhanced as the new method proposed in this paper. Compared with traditional methods, the new method has significantly better contrast enhancement effect on Tableware images. At the same time, compared to the Bookcase image and the Chopsticks frame image, it is obvious that the new method proposed in this paper has better enhancement effect in the experimental image. It is shown that when the pixel value of the image changes, the enhancement effect of the image will also be affected. As the pixel value becomes larger, the color naturalness of the image is better preserved.

Table 3 shows the performance comparison of PQM, RCEF and DSM indicators under different contrast enhancement methods for Tableware image. In Table 3, it is shown that the low RCEF index values are obtained by CLAHE, SSR, Gamma and Median Filter methods, which are 1.2640, 1.0048, 2.3021 and 0.9698 respectively. Obviously, the image enhancement effect of the five traditional methods on PQM index and RCEF index

is not as significant as method we proposed. It is shown that the RCEF index of the self-synaptic FHN neuron is 7.6521 when $PQM = 10.0017$.

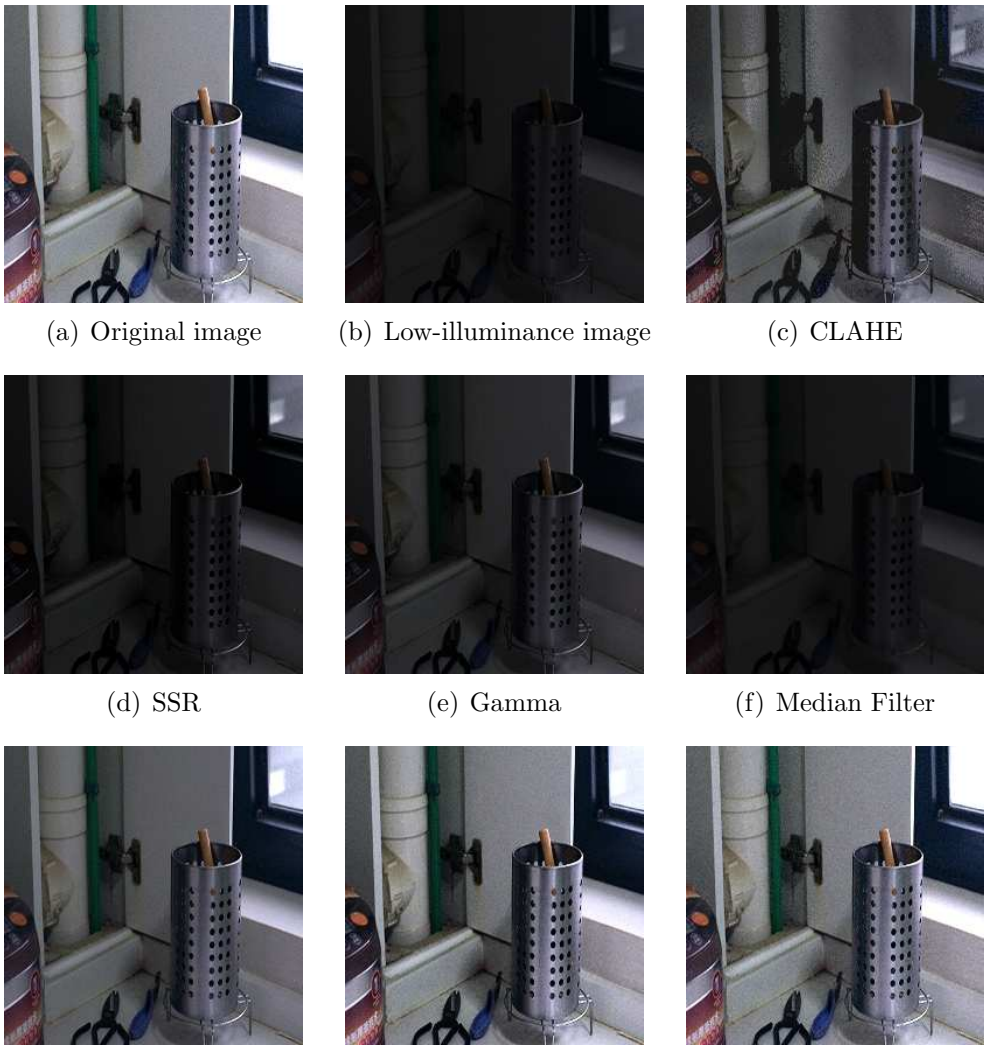

(a) Original image (b) Low-illuminance image (c) CLAHE

(d) SSR (e) Gamma (f) Median Filter

(g) Gaussian Filter (h) FHN (i) Self-synaptic FHN

FIGURE 5. Comparison of Chopsticks frame image with different enhancement methods

TABLE 2. Performance index of Chopsticks frame image under different enhancement methods

Method	Chopsticks frame image (256×256)		
	PQM	RCEF	DSM
CLAHE	10.2791	1.2199	28.5793
SSR	12.1275	3.3986	26.1303
Gamma	11.5653	3.2476	39.0402
Median Filter	11.7578	0.9536	21.2821
Gaussian Filter	10.7936	3.9789	85.1518
FHN	**10.0032**	**5.6788**	**113.8490**
Self-synaptic FHN	**9.9976**	**5.8378**	**123.6339**

(a) Original image (b) Low-illuminance image (c) CLAHE

(d) SSR (e) Gamma (f) Median Filter

(g) Gaussian Filter (h) FHN (i) Self-synaptic FHN

FIGURE 6. Comparison of Tableware image with different enhancement methods

TABLE 3. Performance index of Tableware image under different enhancement methods

Method	Tableware image (512×512)		
	PQM	RCEF	DSM
CLAHE	10.5917	1.2640	29.2226
SSR	13.4434	1.0048	13.4744
Gamma	11.9295	2.3021	37.9187
Median Filter	11.1480	0.9698	23.1776
Gaussian Filter	11.0404	4.9122	114.1453
FHN	**9.9994**	**7.7661**	**129.0997**
Self-synaptic FHN	**10.0017**	**7.6521**	**177.9586**

4. **Conclusion.** In this paper, a self-synaptic FHN neuron model based on ASR is proposed to enhance the contrast of 2D dark and low-contrast images. The Kalman and least mean square (Kalman-LMS) adaptive algorithm is selected to eliminate the input signal interference term and the least square estimation (LSE) adaptive algorithm is selected to obtain the optimal system parameters. The nonlinear iterative method of dynamic adjustment is used to enhance all degree region of low illumination image, and at the same time, the image does not lose its naturalness due to excessive enhancement. Three kinds of images with different pixel sizes are used for contrast enhancement experiments in this paper. The experimental results show that the self-synaptic FHN neuron model is superior to other contrast methods in enhancing the contrast and brightness while preserving the color naturalness of images. And better *DSM* and *RCEF* indicators are obtained with the *PQM* value as close as possible to 10 by the method of this paper compared to the existing methods. The self-synaptic FHN neuron model based on ASR proposed in this paper can be well applied to night detection and biomedical imaging. The number of iterations required to achieve the best enhancement effect and the system optimal parameters required are different in different pixel size images. Therefore, the next goal is that other feasible adaptive algorithms are found and compared with the Kalman-LMS and LSE algorithm for image enhancement of different pixel sizes to obtain the best results. Then the optimal parameters with the best enhancement are obtained with as few iterations as possible.

Acknowledgment. This work is partially supported by the National Natural Science Foundation of China (61501276, 61772294, 61973179), the China Postdoctoral Science Foundation (2016M592139), and the Qingdao Postdoctoral Applied Research Project (2015120).

REFERENCES

[1] W. Zhang, L. Dong, T. Zhang and W. Xu, Enhancing underwater image via color correction and bi-interval contrast enhancement, *Signal Processing: Image Communication*, vol.90, 116030, 2021.
[2] A. M. Chaudhry, M. M. Riaz and A. Ghafoor, Underwater visibility restoration using dehazing, contrast enhancement and filtering, *Multimedia Tools and Applications*, vol.78, no.19, pp.28179-28187, 2019.
[3] M. I. Ashiba, M. S. Tolba, A. S. El-Fishawy and F. E. Abd El-Samie, Hybrid enhancement of infrared night vision imaging system, *Multimedia Tools and Applications*, vol.79, no.9, pp.6085-6108, 2020.
[4] Y. Shin, M. Kim, K.-W. Pak and D. Kim, Practical methods of image data preprocessing for enhancing the performance of deep learning based road crack detection, *ICIC Express Letters, Part B: Applications*, vol.11, no.4, pp.373-379, 2020.
[5] K. Xia, Q. Zhou, Y. Jiang, B. Chen and X. Gu, Deep residual neural network based image enhancement algorithm for low dose CT images, *Multimedia Tools and Applications*, pp.1-24, 2021.
[6] G. A. Baxes, *Digital Image Processing: Principles and Applications*, John Wiley & Sons, Inc., 1994.
[7] J. S. Lim, Two-dimensional signal and image processing, *Englewood Cliffs*, 1990.
[8] K. Zuiderveld, Contrast limited adaptive histogram equalization, *Graphics Gems*, pp.474-485, 1994.
[9] S.-C. Huang, F.-C. Cheng and Y.-S. Chiu, Efficient contrast enhancement using adaptive gamma correction with weighting distribution, *IEEE Transactions on Image Processing*, vol.22, no.3, pp.1032-1041, 2012.
[10] A. Łoza, D. R. Bull, P. R. Hill and A. M. Achim, Automatic contrast enhancement of low-light images based on local statistics of wavelet coefficients, *Digital Signal Processing*, vol.23, no.6, pp.1856-1866, 2013.
[11] J. Yang, Enhancement of LLLIs with improved BCP and matrix completion, *Electronics Letters*, vol.53, no.9, pp.586-588, 2017.
[12] W. Shi, C. Chen, F. Jiang, D. Zhao and W. Shen, Group-based sparse representation for low lighting image enhancement, *2016 IEEE International Conference on Image Processing (ICIP)*, pp.4082-4086, 2016.

[13] D. J. Jobson, Z. Rahman and G. A. Woodell, Properties and performance of a center/surround retinex, *IEEE Transactions on Image Processing*, vol.6, no.3, pp.451-462, 1997.
[14] R. Benzi, A. Sutera and A. Vulpiani, The mechanism of stochastic resonance, *Journal of Physics A: Mathematical and General*, vol.14, no.11, p.453, 1981.
[15] R. Benzi, G. Parisi, A. Sutera and A. Vulpiani, Stochastic resonance in climatic change, *Tellus*, vol.34, no.1, pp.10-16, 1982.
[16] X. Zeng, X. Lu, Z. Liu and Y. Jin, An adaptive fractional stochastic resonance method based on weighted correctional signal-to-noise ratio and its application in fault feature enhancement of wind turbine, *ISA Transactions*, 2021.
[17] V. Sorokin and I. Demidov, On representing noise by deterministic excitations for interpreting the stochastic resonance phenomenon, *Philosophical Transactions of The Royal Society A Mathematical Physical and Engineering Sciences*, vol.379, no.2192, 20200229, 2021.
[18] F. Guo, X. Wang, M. Qin, X. Luo and J. Wang, Resonance phenomenon for a nonlinear system with fractional derivative subject to multiplicative and additive noise, *Physica A: Statistical Mechanics and Its Applications*, vol.562, 125243, 2021.
[19] J. Yu, L. Zhao, H. Yu and C. Lin, Barrier Lyapunov functions-based command filtered output feedback control for full-state constrained nonlinear systems, *Automatica*, vol.105, pp.71-79, 2019.
[20] J. Yu, P. Shi and L. Zhao, Finite-time command filtered backstepping control for a class of nonlinear systems, *Automatica*, vol.92, pp.173-180, 2018.
[21] S. Ikemoto, Noise-modulated neural networks for selectively functionalizing sub-networks by exploiting stochastic resonance, *Neurocomputing*, vol.448, pp.1-9, 2021.
[22] C. Ma and J. Ao, Nonlinear average stochastic resonance for image enhancement, *The International Journal of Electrical Engineering & Education*, DOI: 10.1177/0020720920940613, 2020.
[23] A. R. Bulsara, Tuning in to noise, *Physics Today*, vol.49, no.3, pp.39-45, 1996.
[24] Z. Khan, J. Ni, X. Fan and P. Shi, An improved k-means clustering algorithm based on an adaptive initial parameter estimation procedure for image segmentation, *International Journal of Innovative Computing, Information and Control*, vol.13, no.5, pp.1509-1525, 2017.
[25] J. Zhao, Y. Ma, Z. Pan and H. Zhang, Research on image signal identification based on adaptive array stochastic resonance, *Journal of Systems Science and Complexity*, pp.1-15, 2021.
[26] N. Wang and A. Song, Parameter-induced logical stochastic resonance, *Neurocomputing*, vol.155, pp.80-83, 2015.
[27] L. Xiao, R. Bajric, J. Zhao, J. Tang and X. Zhang, An adaptive vibrational resonance method based on cascaded varying stable-state nonlinear systems and its application in rotating machine fault detection, *Nonlinear Dynamics*, vol.103, no.1, pp.715-739, 2021.
[28] C. Wu, Z. Wang, J. Yang, D. Huang and M. A. F. Sanjuán, Adaptive piecewise re-scaled stochastic resonance excited by the LFM signal, *The European Physical Journal Plus*, vol.135, no.1, p.130, 2020.
[29] D. Zhou, D. Huang, J. Hao, Y. Ren, P. Jiang and X. Jia, Vibration-based fault diagnosis of the natural gas compressor using adaptive stochastic resonance realized by generative adversarial networks, *Engineering Failure Analysis*, vol.116, 104759, 2020.
[30] B.-Q. Fan, Y.-J. Zhang, Y. He, K. You, M.-Q. Li, D.-Q. Yu, H. Xie and B.-E. Lei, Adaptive monostable stochastic resonance for processing UV absorption spectrum of nitric oxide, *Optics Express*, vol.28, no.7, pp.9811-9822, 2020.
[31] J. Li, X. Wang and H. Wu, Rolling bearing fault detection based on improved piecewise unsaturated bistable stochastic resonance method, *IEEE Transactions on Instrumentation and Measurement*, vol.70, pp.1-9, 2020.
[32] R. Chouhan, R. K. Jha and P. K. Biswas, Enhancement of dark and low-contrast images using dynamic stochastic resonance, *IET Image Processing*, vol.7, no.2, pp.174-184, 2013.
[33] U. A. Nnolim, Single image de-hazing using adaptive dynamic stochastic resonance and wavelet-based fusion, *Optik*, vol.195, 163111, 2019.
[34] M. Hussain and M. Rehan, Nonlinear time-delay anti-windup compensator synthesis for nonlinear time-delay systems: A delay-range-dependent approach, *Neurocomputing*, vol.186, pp.54-65, 2016.
[35] A. Nomura, Initial conditions of reaction-diffusion algorithm designed for image edge detection, *International Conference on Image Analysis and Recognition*, pp.246-251, 2019.
[36] M. Rehan, K.-S. Hong and M. Aqil, Synchronization of multiple chaotic FitzHugh-Nagumo neurons with gap junctions under external electrical stimulation, *Neurocomputing*, vol.74, no.17, pp.3296-3304, 2011.

[37] L. Shi, D. Li, X. Li and X. Wang, Dynamics of stochastic FitzHugh-Nagumo systems with additive noise on unbounded thin domains, *Stochastics and Dynamics*, vol.20, no.3, 2050018, 2020.
[38] S. Li and J. Huang, Non-Gaussian noise induced stochastic resonance in FitzHugh-Nagumo neural system with time delay, *AIP Advances*, vol.10, no.2, 025310, 2020.
[39] W. Ke, Q. He and Y. Shu, Functional self-excitatory autapses (auto-synapses) on neocortical pyramidal cells, *Neuroscience Bulletin*, vol.35, no.6, pp.1106-1109, 2019.
[40] Y. Li, G. Schmid, P. Hänggi and L. Schimansky-Geier, Spontaneous spiking in an autaptic Hodgkin-Huxley setup, *Physical Review E*, vol.82, no.6, 061907, 2010.
[41] Y. Xu, Y. Guo, G. Ren and J. Ma, Dynamics and stochastic resonance in a thermosensitive neuron, *Applied Mathematics and Computation*, vol.385, 125427, 2020.
[42] A. V. Andreev and A. N. Pisarchik, Mathematical simulation of coherent resonance phenomenon in a network of Hodgkin-Huxley biological neurons, *Saratov Fall Meeting 2018: Computations and Data Analysis: from Nanoscale Tools to Brain Functions*, vol.11067, 1106708, International Society for Optics and Photonics, 2019.
[43] T. C. Gard, *Introduction to Stochastic Differential Equations*, Marcel Dekker Ins., New York, 1998.
[44] J. E. Parker and K. M. Short, Sigmoidal synaptic learning produces mutual stabilization in chaotic FitzHugh-Nagumo model, *Chaos: An Interdisciplinary Journal of Nonlinear Science*, vol.30, no.6, 063108, 2020.
[45] D. Brown, J. Feng and S. Feerick, Variability of firing of Hodgkin-Huxley and FitzHugh-Nagumo neurons with stochastic synaptic input, *Physical Review Letters*, vol.82, no.23, 4731, 1999.
[46] L. Xu, F. Duan, D. Abbott and M. D. McDonnell, Optimal weighted suprathreshold stochastic resonance with multigroup saturating sensors, *Physica A: Statistical Mechanics and Its Applications*, vol.457, pp.348-355, 2016.
[47] A. H. Sayed and T. Kailath, A state-space approach to adaptive RLS filtering, *IEEE Signal Processing Magazine*, vol.11, no.3, pp.18-60, 1994.
[48] D. P. Mandic, S. Kanna and A. G. Constantinides, On the intrinsic relationship between the least mean square and Kalman filters [lecture notes], *IEEE Signal Processing Magazine*, vol.32, no.6, pp.117-122, 2015.
[49] E. Itzcovich, M. Riani and W. G. Sannita, Stochastic resonance improves vision in the severely impaired, *Scientific Reports*, vol.7, no.1, pp.1-8, 2017.
[50] N. Gupta and R. K. Jha, Enhancement of dark images using dynamic stochastic resonance with anisotropic diffusion, *Journal of Electronic Imaging*, vol.25, no.2, 023017, 2016.
[51] Z. Wang, H. R. Sheikh and A. C. Bovik, No-reference perceptual quality assessment of JPEG compressed images, *Proc. of International Conference on Image Processing*, vol.1, pp.I-I, 2002.
[52] J. Mukherjee and S. K. Mitra, Enhancement of color images by scaling the DCT coefficients, *IEEE Transactions on Image Processing*, vol.17, no.10, pp.1783-1794, 2008.
[53] N. Gupta, R. K. Jha and S. K. Mohanty, Enhancement of dark images using dynamic stochastic resonance in combined DWT and DCT domain, *2014 9th International Conference on Industrial and Information Systems (ICIIS)*, pp.1-6, 2014.

Author Biography

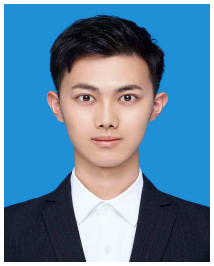

Dongcheng Wang received the B.S. degree from Qufu Normal University, Rizhao, China, in 2019. He is currently pursuing the M.S. degree at Qingdao University, Qingdao, China. His research interests are nonlinear signal processing and image processing.

Yumei Ma received B.Eng. and M.Eng. degrees from Shandong University in 2002 and 2006 respectively and D.Eng. degree from Qingdao University in 2014. She is an associate professor at the College of Computer Science and Technology of Qingdao University. Her research interests are nonlinear signal processing and image processing. She has presided over one National Natural Science Foundation project and two provincial and ministerial research projects. She has published more than 50 academic papers.

Zhenkuan Pan received Ph.D. degree from Shanghai Jiao Tong University in 1992 and B.E. degree from Northwestern Polytechnical University in 1987 respectively. He is a professor in the College of Computer Science and Technology, Qingdao University. He has authored and co-authored more than 300 academic papers in the areas of computer vision and dynamics. His research interests include variational models of image and geometry processing, multibody system dynamics, etc.

Ning Zhang received the B.S. degree from Qingdao Institute of Technology, Qingdao, China, in 2019. He is currently pursuing the M.S. degree at Qingdao University, Qingdao, China. His research interests are nonlinear signal processing and image processing.